2017 IEEE International Conference on Systems, Man, and Cybernetics (SMC)
Banff Center, Banff, Canada, October 5-8, 2017

Generating a Fuzzy rule-based Brain-state-drift Detector by Riemann-Metric-based Clustering

Yu-Cheng Chang[1], Yu-Kai Wang[1], Dongrui Wu[2], Chin-Teng Lin[1]
[1] Centre for Artificial Intelligence, University of Technology Sydney, Australia
[2] DataNova, NY USA

***Abstract*— Brain-state drifts could significantly impact on the performance of machine-learning algorithms in brain computer interface (BCI). However, less is understood with regard to how brain transition states influence a model and how it can be represented for a system. Herein we are interested in the hidden information of brain state-drift occurring in both simulated and real-world human-system interaction. This research introduced the Riemann metric to categorize EEG data, and visualized the clustering result so that the distribution of the data can be observable. Moreover, to defeat subjective uncertainty of electroencephalography (EEG) signals, fuzzy theory was employed. In this study, we built a fuzzy rule-based brain-state-drift detector to observe the brain state and imported data from different subjects to testify the performance. The result of the detection is acceptable and shown in this paper. In the future, we expect that brain-state drifting can be connected with human behaviors via the proposed fuzzy rule-based classification. We also will develop a new structure for a fuzzy rule-based brain-state-drift detector to improve the detection accuracy.**

I. Introduction

Brain states provides informative value to human performance modeling, uncertainty estimation, and human-system interaction. A brain state is defined in this paper as intermediate representation of features (e.g., independent components, power spectral, etc.) derived from electroencephalography (EEG) signals. Herein we are particularly interested in the attentional and cognitive states, which are always changing or drifting. Brain-state drifts could significantly impact on the performance of machine-learning algorithms in brain computer interface (BCI). Detecting state drifts is able to help us understand when and why a machine learning algorithm for human performance modeling deteriorates, and also enable us to design more appropriate and efficient state-based machine learning approaches. The brain state can also leverage to model human performance, estimate uncertainty, and build interactive system.

Previous studies associated with the brain state-drift majorly discovered the active brain sources according to the extremely good and poor behaviors. For example, the researchers applied Morlet-wavelet time-frequency analysis to classify human implicit intentions of agreement versus disagreement [1]. Lin *et al.* implemented EEG-based drowsiness prediction system using self-organizing neural fuzzy inference network (SONFIN) [2]. However, the underlying brain sources and their interactions might differ dramatically under different brain states from time to time. Therefore, studying the dynamic changes of the brain states is crucial. In this study, we investigated the EEG dynamics in one long-duration experiments in which the participants performed the attentional. There were many works employing fuzzy theory to handle subjective uncertainty of EEG signals. the authors of [2] used SONFIN to achieve subject-dependent drowsiness prediction. TSK-type fuzzy system was introduced to recognize epileptic EEG signals in paper [3]. The interval type-2 fuzzy used in study [4] is also a good technique to handle uncertainty. Herein we are interested in hidden information of brain state-drift occurring in both simulated and real-world human-system interaction. This aim of this study is to detect the changes of brain state according to one-second EEG signal. Moreover, biological signals of human beings change depending on the body condition (e.g. metal condition, physical condition and etc.); in other words, biological signals of human beings, such as EEG signals, have high level of subjective uncertainty. Meanwhile, fuzzy theory constitutes an efficient way to deal with subjective uncertainty; it offers a mathematic model to translate the subjective human information of the real processes. Accordingly, Fuzzy neuro network (FNN) [5] was introduced to classify transition states of EEG signals.

Yu-Cheng Chang, Yu-Kai Wang and Chin-Teng Lin are with the Computational Intelligence and Brain Computer Interface (CIBCI) lab, University of Technology, Sydney, Australia (E-mail: fred750705@gmail.com, YuKai.Wang@uts.edu.au and chintenglin@gmail.com)

II. Methods

A. Brain-state-drift detection framework

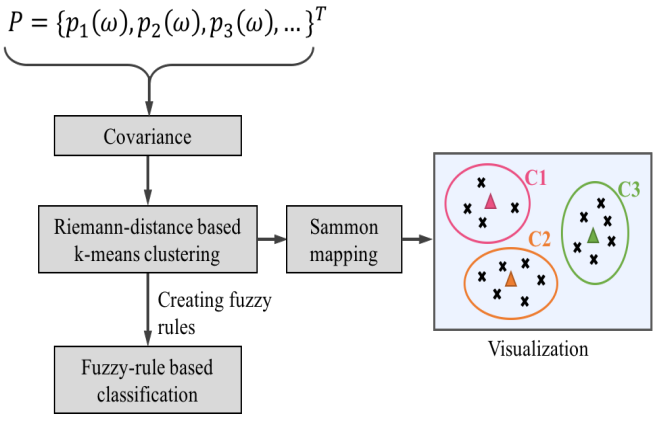

Figure 1. The block diagram of fuzzy rule-based brain-state-drift detection. The extracted feature of EEG signals were clustered through Riemann-distance-based k-means clustering. The Sammon mapping was then introduced to visualize the clustering results.

978-1-5386-1645-1/17/$31.00 ©2017 IEEE

Figure 1 interprets the procedure of state-drift detection framework. To automatically cluster data, Riemann-distance based k-means, which is an unsupervised clustering approach, was used. The Riemann distance was adapted to measure the distances between each datum and the centers of each clustering [6]. In many clustering problem, Euclidean distance was widely used. However, the features in this study were power spectral densities. Each power spectral density matrix could be described as a point in the Riemann manifold, which means that clustering of similar and dissimilar EEG signal sets were more separable. The EEG data in the same class should be more compact [7]. Hence, Euclidean metrics was not suitable in the EEG analysis with high dimension.

After data clustering, the clustering result can be applied to create a fuzzy rule-based classifier (FRC), which is able to predict brain states with input EEG data captured before the event occurs. We therefore can establish a model, state-drift detection framework, to observe if brain state is drifting or not. Additionally, we would like to observe clusters and data distributions to investigate brain state more profoundly, which would assist to interpret the clustering results. However, it is impossible to directly observe transaction and data distribution due to the high dimension of extracted feature. A nonlinear mapping approach, such as Sammon mapping [8], was introduced to visualize the results of clustering therefore. Sammon mapping enable structure of high dimension data to be preserve in low dimension space by approximating corresponding inter-point distances in low dimension space [9].

B. Clustering and Visualization

In this study, we used *k*-means clustering approach to divide EEG data into *K* clusters in which each datum belongs to the cluster with the smallest distance to the cluster center. The distance for measurement is the Riemann distance. The Riemann distance between P_n and P_m is

$$d_R(P_n, P_k) = \sqrt{tr[(\log P_n - \log P_k)^2]} = \sqrt{tr\left[\left(\log P_k^{-1/2} P_n P_k^{-1/2}\right)^2\right]} = \sqrt{\sum_{i=1}^{M} (log\ \lambda_i)^2} \quad (1)$$

where λ_i are the eigenvalues of $P_k^{-1}P_n$, $P_k$is the center of *k*-th cluster. The center of a cluster can be find as following:

$$C_i = arg\ \min d_R(P_n, P_k) \quad (2)$$

The algorithm of *k*-means clustering consists of the following steps.

1) *K* centers are randomly chosen from the dataset.
2) Each datum is assigned a center with the closet distance to the center.
3) The approximate center of each cluster is recalculated from the belonging points.
4) The second and third steps are repeated until the proper clustering is generated.

When the proper clustering is obtained, the result of clustering can be mapped from high dimension to low dimension (e.g. two-dimension space) using the Sammon mapping.

To project high-dimension data onto two-dimension space, the inter-point Riemann distances in high-dimension space $d_{ij} = d_R(P_i, P_j)$ and the corresponding inter-point Euclidean distances in two-dimension space $\hat{d}_{ij} = d(\hat{P}_i, \hat{P}_j)$ have to be approximated by the error criterion of the Sammon mapping.

We mapped all cluster centers and all trial of data from high-dimension space to two-dimension space so that the we can simply observe distributions of data.

The error criterion of the Sammon mapping used here is as follows:

$$E = \frac{1}{\lambda}\sum_{i=1}^{K-1}\sum_{j=i+1}^{K}\frac{d_R(P_i, P_j) - d(\hat{P}_i, \hat{P}_j)}{d_R(P_i, P_j)}, \quad (3)$$

where *K* is the total number of data and the clustering centers, $d_R(.)$ is the Reimman distance and $d(.)$ is the Euclidean distance. The error criterion considers the the Reimman distance as inter-point distance in high dimension since the clusters were generated based on the Riemann distance. By doing so, the data distribution in the tangent space can be directly observed.

C. Fuzzy-rule based classification

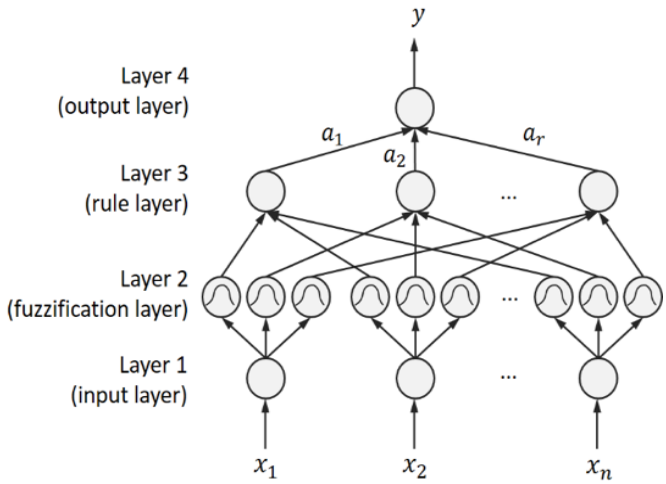

Figure 2. Architecture of fuzzy neural network (FNN). There are four layers, including input layer, fuzzification layer, rule layer and output layer in FNN. The mean of each fuzzy set was built based on clustering center.

To establish a brain-state-drift detector able to defeat subjective uncertainty of EEG signals, we employ fuzzy neural network to classify incoming data. The architecture of fuzzy neural network is shown in Figure 2. There are four layers in an FNN described as follows.

Layer 1 (input layer): the nodes in this layer transmit input data to next layer. A normalization operation is usually introduced in this layer for input range unification.

Layer 2 (fuzzification layer): input data is fuzzified in this layer. Each node represents one fuzzy set and evaluates a membership function. The membership function can be a Gaussian membership function.

Layer 3 (rule layer): each node represents a fuzzy rule which corresponds to one firing strength for defuzzification. To obtain firing strength, the AND operation is adopted.

Layer 4 (output layer): The connection weights between layer 3 and layer 4 are the consequent values. Each node calculates one output variable using weighted average method.

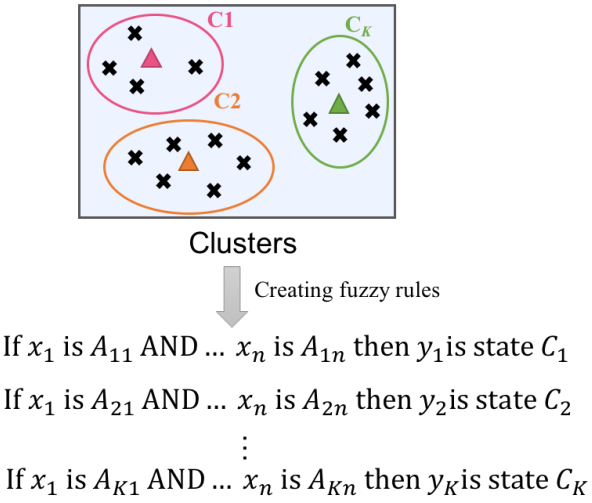

Figure 3. Each fuzzy rule can be derived from corresponding cluster. the center of a cluster constructs the mean of each fuzzy set in a rule. The consequence of each rule is the index of cluster representing a particular state.

The fuzzy rules were built depending on the clustering results, as shown in figure 3. More specifically, each clustering center was treated as the means of Gaussian membership functions of each fuzzy rule, and the consequences of each fuzzy rule were the indexes of corresponding clusters representing the brain states. The widths of Gaussian membership functions were optimized by gradient descent algorithm. The output of the classifier is a particular state of an input datum. With this framework, the state of EEG signal can be discriminated. The brain-state-drift is able to be detected as well.

D. Collecting EEG data

There were six neurologically healthy volunteers participating the experiment (20-28 years of age; mean age: 24.3 years; all males). We utilized a lane-keeping driving task in the driving experiment. This driving experiment was conducted in National Chiao Tung University, Hsinchu, Taiwan [10]. One real car was mounted on the virtual-reality-based scenario. The participants only needed to keep the car along the cruising lane while the car was deviating randomly for one hour. In the experiment, the car was linearly drifted from the cruising lane either to the curb (right) or the opposite lane (left) as shown in Figure 4. A is the point when the deviation appeared. B is the point when the participant began to tune the the steering wheel. The interval between each two deviation events happening was set to 7 – 12 seconds. The participants were asked to driving for one hour continuously.

In this simulation, the number of training data was 300, each subject provides around 50 trials including the 25 trials with drowsiness label and 25 with alertness label. The number of cluster was set to six. Therefore, there were six rules in the FRC, and the outputs would be particular index of the six states.

When the deviation appeared, the participants were instructed to quickly steer the car back to the cruising lane by turning the steering wheel. After turning the steering wheel and returning to the cruising lane, small corrections for precise alignment were prohibited. The latency from the onset of deviation to the onset of turning steering wheel was defined as the reaction times (RTs) for driving task.

Two classes, drowsiness and alertness were defined in this experiment. All RTs from every subject were sorted first. To define drowsiness and alertness, the mean value of top 10% RTs (fastest) was the baseline. RT values which are smaller than 1.2 times of the baseline are defined as alert states (normal driving). RT values which are larger than 2 times of the baseline are defined as drowsy states (hitting the curb or opposite lane).

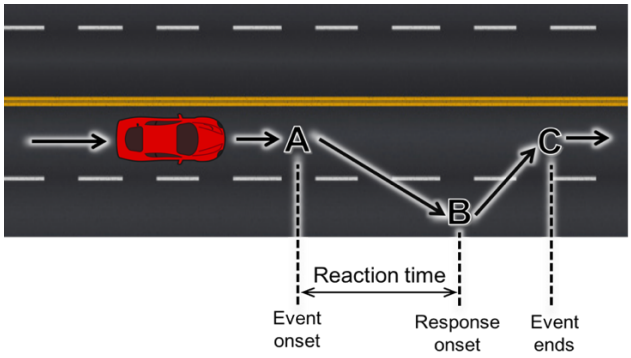

Figure 4. The lane-keeping driving task. The car drifts to left or right randomly, and the participants need to keep the car in the third lane through turning the steering wheel.

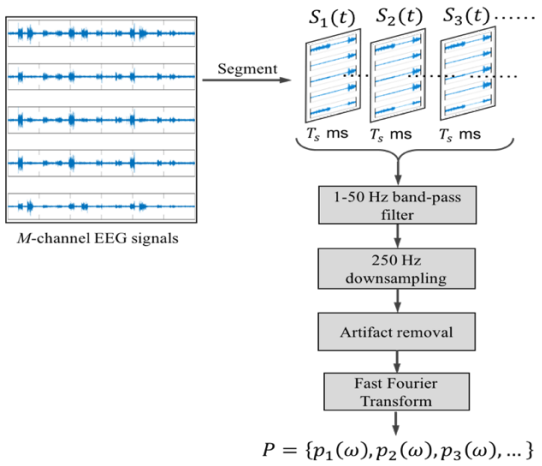

Figure 5. The block diagram of feature extraction for brain-state-drift detection framework.

Figure 5 describes the scheme of feature extraction for brain-state-drift detection framework. The EEG data were epoched from -1000 to 0 ms according to the event onset. Then, each epoched data were filtered by a 1-50 Hz band-pass filter impulse response (FIR) filter to remove the DC-drifts and high-frequency artifacts with re-sampling at 250 Hz. The artifact free EEG data were transferred from time domain to frequency domain using Fast Fourier Transform (FFT). The spectral magnitudes of delta (1-3 Hz), theta (4-7 Hz), alpha (8-13 Hz), and low beta (14-20 Hz) were calculated. We exploited the mean value of spectral magnitudes with top 10% RTs (fastest) as the spectral baseline. Each epoched data were subtracted by the baseline for normalization. Finally, channels of frontal lobe (e.g. F3, FZ and F4), parietal lobe (e.g. P3, PZ and P4) and occipital lobe (e.g. O1, OZ and O2) were selected as input channels. The dimension of each sample therefore was 120 (4 bands * 9 channels).

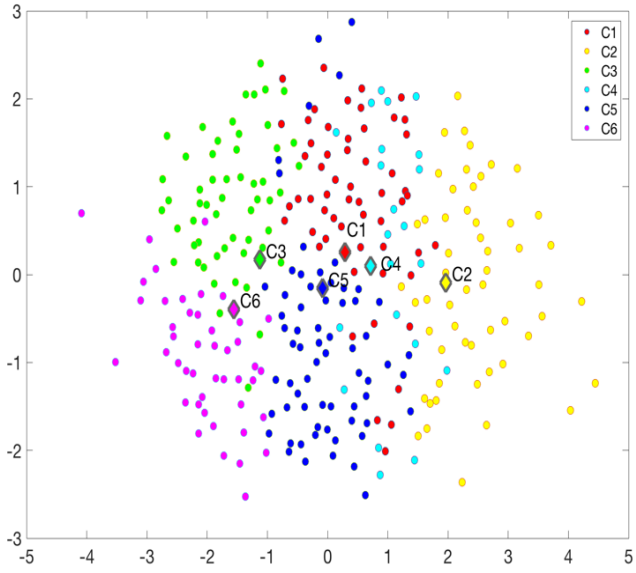

Figure 6. Clustering result presented with Sammon mapping on 2-D space. The number of cluster is six, each cluster is labeled with different color. The diamond shapes represent centers of each cluster.

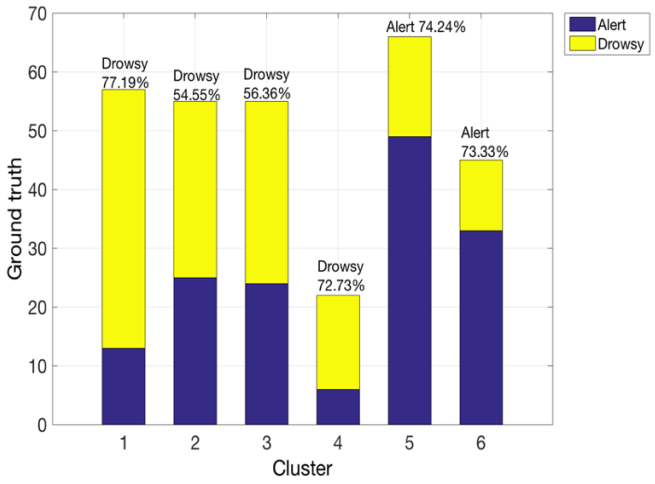

Figure 7. the distribution of the drowsiness and alertness class in each cluster. The number on the top of each bar represents the percentage of the dominated class.

III. Result and Discussion

Figure 6 reveals the clustering results, and each point was projected from high dimension onto two dimension using Sammon mapping. Figure 6 demonstrates that the Sammon mapping is capable of transferring the distribution of each cluster in the tangent space onto two-dimensional Euclidean space. This projection was helpful to observe and interpret the EEG data. According to the clustering distribution shown in figure 6, the data belongs C_5 and C_6 were most with drowsiness label. Meanwhile, C_1 and C_4 contained most alertness-labeled data. Others, C_2 and C_4, both contained drowsiness-labeled data slightly more than alertness-labeled data. Additionally, figure 6 shows of the drowsiness and alertness class in each cluster. According to the distribution of the data and the class shown in Figure 6 and Figure 7, we can treat C_5 and C_6 as both representative states for drowsiness since the visualized data C_5 and C_6 in figure 6 were adjacent and not confused, and the dominated class were both alertness. On the other hand, C_1 can be treated as representative states for alertness as it had the same condition with C_5 and C_6 in Figure 5, and Figure 6 shows their dominated class was drowsiness. Except that, the visualized data of C_4 in Figure 5 was incompact, although it contained high rate of drowsiness class, it cannot be treated as representative states.

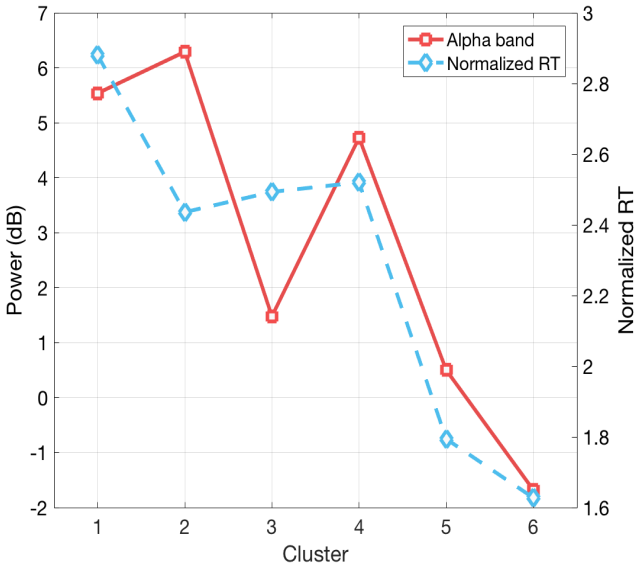

Figure 8. Changes of alpha activity and normalized reaction time over each cluster. The right y-axis represents power spectra of alpha band. The left y-axis represents value of normalized reaction time.

Figure 8 shows a strong correlation between alpha activities and normalized RT changes over each cluster. In the figure 8, C_6 had lowest alpha activities and RT value, which demonstrated that C_6 is a robust state for high-level alertness. The alpha activity and RT value of C_5 both stood at the second place. Thus, C_5 can be treated as a moderate-level alertness state. Moreover, the normalized RT values of C_3 and C_4 were similar; C_3 was 2.49 and C_4 was 2.52. The alpha band of C_3, however, was lower than of C_4. Therefore, we defined these two clusters were drifting states. The drifting state C_3 was a state changing from moderate-level alertness to drowsiness. Besides, C_2 had both high-level alpha and beta activity, as shown in Figure 9 and Figure 10 respectively. This means C_2 is a fighting-fatigue state. Finally, C_1 can be treated as robust state for drowsiness since it had high-level alpha activity and largest normalized RT value.

With the interpretation above, we therefore can exploit the clustering result to build an FCR for brain-state detection. For example, the variables in center of C_1 were assigned to rule 1 as the mean values of Gaussian membership function. The corresponding consequence then was C_1. By doing so, we can analyze the brain states from other different subjects via built FCR. More specifically, if states are classified to C_5 or C_6, the states can be treated as alertness. If states are classified to C_1, the states can be treated as drowsiness. Finally, if states are classified to C_4 the states can be treated as drifting states.

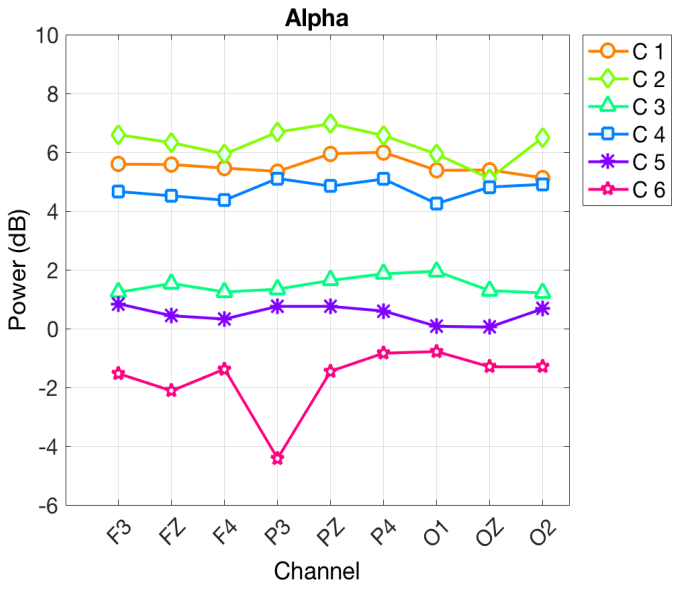

Figure 9. Average power spectra of alpha wave of each channel over each cluster.

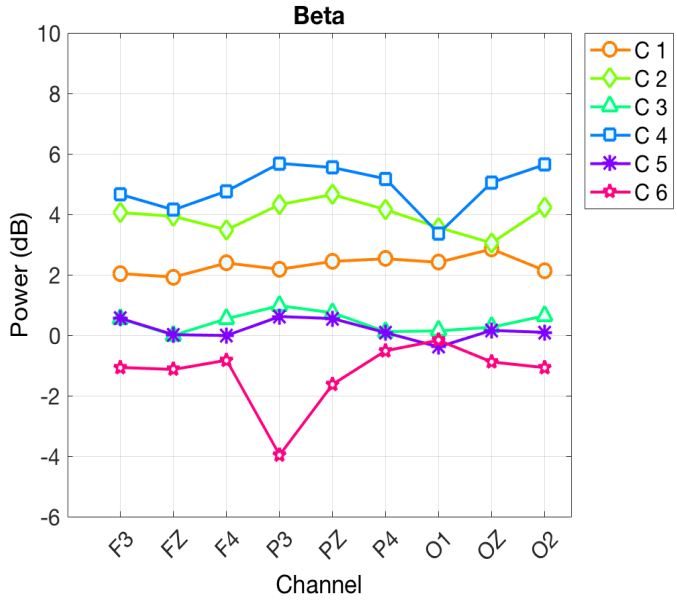

Figure 10. Average power spectra of beta wave of each channel over each cluster.

IV. Conclusion

In this study, we built one FRC for detecting brain-state-drift during long-term driving. In particular, Sammon mapping was applied to visualize the high dimension data, which was able to categorize data most with the same label together. The visualization also assisted to interpret the clustering results. This classifier was tested with the EEG signals recorded from continuous driving experiment with different attentional requirements. The results showed that the FRC built with data from the six subjects was capable of classifying the data from another different subject. However, more states should be observed to represent the different attentional requirements. In

the near future, we will conduct simulations with more different subjects for leave-one-subject-out cross-validation. we expect that this classifier can leverage to monitor state changes from EEG signals. We also age to connect the human behaviors and the changes of brain state through the proposed fuzzy rule-based classification. Furthermore, a new structure of fuzzy rule-based brain-state-drift detector will be developed to improve the classification performance.

ACKNOWLEDGEMENT

This work was supported in part by the Australian Research Council (ARC) under discovery grant DP150101645, in part by Central for Artificial Intelligence, UTS, Australia, and in part by the Aiming for the Top University Plan of National Chiao Tung University, the Ministry of Education, Taiwan, under Contract 104W963. Research was also sponsored in part by the Army Research Laboratory and was accomplished under Cooperative Agreement Number W911NF-10-2-0022.

REFERENCES

[1] S. Dong, B. Kim and S. Lee, "EEG-Based Classification of Implicit Intention During Self-Relevant Sentence Reading", *IEEE Transactions on Cybernetics*, vol. 46, no. 11, pp. 2535-2542, 2016.

[2] F. Lin, L. Ko, C. Chuang, T. Su and C. Lin, "Generalized EEG-Based Drowsiness Prediction System by Using a Self-Organizing Neural Fuzzy System", *IEEE Transactions on Circuits and Systems I: Regular Papers*, vol. 59, no. 9, pp. 2044-2055, 2012.

[3] Y. Jiang, Z. Deng, F. Chung, G. Wang, P. Qian, K. Choi and S. Wang, "Recognition of Epileptic EEG Signals Using a Novel Multiview TSK Fuzzy System", *IEEE Transactions on Fuzzy Systems*, vol. 25, no. 1, pp. 3-20, 2017.

[4] A. Khasnobish, A. Konar, D. Tibarewala and A. Nagar, "Bypassing the Natural Visual-Motor Pathway to Execute Complex Movement Related Tasks Using Interval Type-2 Fuzzy Sets", *IEEE Transactions on Neural Systems and Rehabilitation Engineering*, vol. 25, no. 1, pp. 91-105, 2017.

[5] Wang, J. S., & Lee, C. S. G. (2002), "Self-adaptive neuro-fuzzy inference systems for classification applications," *IEEE Trans. on Fuzzy Systems*, vol. 10, no. 6, 790–802.

[6] A. Barachant, S. Bon, M. Congedo and C. Jutten, "Common Spatial Pattern revisited by Riemannian geometry", *2010 IEEE International Workshop on Multimedia Signal Processing*, 2010.

[7] Yili Li, Kon Max Wong and H. deBruin, "EEG signal classification based on a Riemannian distance measure", *2009 IEEE Toronto International Conference Science and Technology for Humanity (TIC-STH)*, 2009.

[8] J. Sammon, "A Nonlinear Mapping for Data Structure Analysis", *IEEE Transactions on Computers*, vol. -18, no. 5, pp. 401-409, 1969.

[9] J. Abonyi and R. Babuska, "FUZZSAM - visualization of fuzzy clustering results by modified Sammon mapping", *2004 IEEE International Conference on Fuzzy Systems* (IEEE Cat. No.04CH37542).

[10] Y. Liu, Y. Lin, S. Wu, C. Chuang and C. Lin, "Brain Dynamics in Predicting Driving Fatigue Using a Recurrent Self-Evolving Fuzzy Neural Network", *IEEE Transactions on Neural Networks and Learning Systems*, vol. 27, no. 2, pp. 347-360, 2016.